AN ACCURATE AND AUTOMATIC COLOR CORRECTION METHOD FOR DIGITAL FILMS BASED ON A PHYSICAL MODEL

Quoc Bao DO, Azeddine BEGHDADI, Marie LUONG

L2TI/ Université Paris 13, France

ABSTRACT

A new method for detecting and correcting color-mismatch in digital film is proposed. This method is based on a physical model which accounts for the absorption of light by the different layers of the film. The whole process consists of three sequential stages. Based on the physical model, a robust optical flow method which is invariant to color change is proposed. From the computed flow field, a detection and restoration of distortion regions can be achieved. The obtained results confirm the efficiency of the proposed method.

1. INTRODUCTION

In the film post-production, the color fidelity of the original images is of great importance. Indeed, the release prints (RP) are produced from the original negative (ON) through two intermediate elements called Interpositive (IP) and Internegative (IN) [1] (see Fig.1 – red arrow). The principle of film printing is to form an image onto a virgin film (called raw stock) from a developed one by exposing it to a light source. This light consists of three components red, green and blue beams. The two films should move at the same speed in front of the light. It is important to notice that, unlike in IP-IN and IN-RP steps where the light setting is constant during the entire printing process, this light is adapted to each shot in ON-IP step by adjusting the intensity of each beam. This type of color adjustment is called color-timing light. The use of this adapted light has several goals [1-3] (i) variations in exposure and lighting between different shots will be evened out to provide a continuity of colour throughout a film, (ii) the colour of some objects may need to be reproduced exactly, (iii) the appropriate mood must be created, for example, warm balance for romantic scenes, darker for stormy effects and so on. Although the printing speed is slow during this step, IP may suffer from a particularly undesirable artifact, mostly visible at shot boundary due to the mismatch of color-timing light. An example of this mismatch is shown in Fig.2. The bottom of the last frame a_n of shot A and the top of the 1st frame b_1 of shot B is exposed to an inadequate light corresponding to the transition from the first color setting ($R_1G_1B_1$) to the second one ($R_2G_2B_2$). Consequently, in IP, there is a color variation that can be observed on the top of the degraded frame b_1 when compared to the reference b_2 of shot B (similar remark for the bottom of frame a_n of shot A). This undesirable degradation through IN affects the quality of RP. In modern scheme, some digital intermediates are also used in the film post-processing (green arrow). An example of the default is shown in Fig.6a,b where the top of the degraded frame is greener than in the reference one (see zooms in Fig.13a,b and Fig.14a,b for more details).

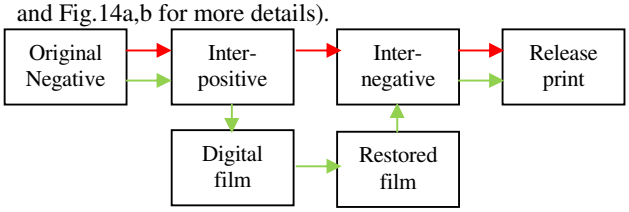

Figure 1-Film post-processing procedure

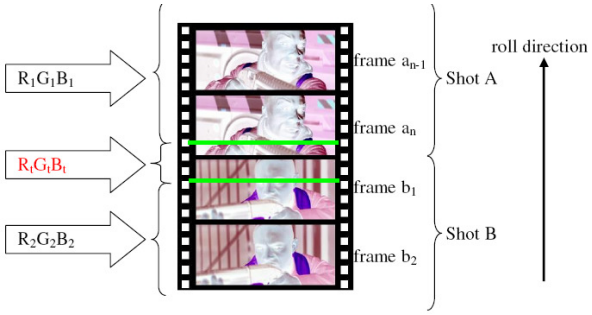

Figure 2: Example of mismatching color-timing light

In [4], a method based on histogram specification is proposed to cope with this issue. However, this method cannot accurately detect degraded zone when high motion presents and results in false colors in occluded regions. In this paper, a physical model describing the different steps from ON to digital film (DF) is proposed and used for restoring the film. To cope with the color-mismatch that may result in the case of motion, a new optical flow method which is robust to color change is proposed. The computed flow field is then used to align the degraded image with the reference one in order to estimate the color degradation. The restoration is then based on this spatio-temporal information.

The paper is organized as follows: the physical model is presented in section 2 followed by the proposed optical flow algorithm is section 3, degradation detection and image restoration schemes are described in section 4. The experimental results are reported in section 5 followed by a conclusion in section 6.

2. PHYSICAL MODEL

To precise, let us recall that there are mainly three steps from ON to DF. First, exposed film (EF) is obtained by exposing ON to light, then the development of EF yields IP and finally DF results from the scan of IP. A film structure can be considered a set of three layers, i.e., red, green and

blue sensitive layers which form cyan, magenta, yellow dye, respectively. In the 1st step (see Fig.3), the spectral energy $E(\lambda)$ of the exposed light is composed of 3 beams, i.e. red $E_r(\lambda)$, green $E_g(\lambda)$ and blue $E_b(\lambda)$ which are respectively adjusted by three weighting factors α_r, α_g, α_b:

$$E(\lambda) = \alpha_r E_r(\lambda) + \alpha_g E_g(\lambda) + \alpha_b E_b(\lambda) \quad (1)$$

According to Beer-Lambert law [5], the transmitted light $ET(\lambda)$ is as follows:

$$ET(\lambda) = E(\lambda)\tau_n(\lambda) \quad (2)$$

where $\tau_n(\lambda)$ is the transmittance defined as follows:

$$\tau_n(\lambda) = 10^{-(c_n D_c(\lambda) + m_n D_m(\lambda) + y_n D_y(\lambda))z} \quad (3)$$

where c_n, m_n, y_n are dye density (the subscript 'n' indicates negative) and $D_c(\lambda)$, $D_m(\lambda)$, $D_y(\lambda)$ are spectral density of cyan, magenta, yellow layer respectively, z is the thickness of the emulsion. The raw stock exposed to this transmitted light produces latent images in EF. For the sake of conciseness, we express the equations only for the red-sensitive layer (similar results can be derived for the green and blue ones). The exposure level is as follows:

$$X_r = t_o \int_w ET(\lambda) L_r(\lambda) d\lambda \quad (4)$$

where t_o is the exposure time, $L_r(\lambda)$ is the spectral sensitivity (film speed) of this layer and w is the wavelength of visible light.

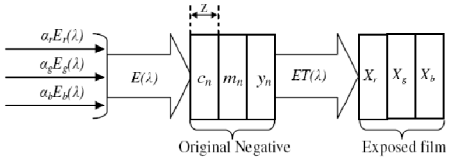

Figure 3 – From original negative to exposed film

In the 2nd step (see Fig.4a), the EF is passed through a development process to yield visible images. This process is modelled by H-D curve [1,3,6] (Fig.4b). This function describes the relation between the exposure level X_r, X_g, X_b and the dye density c_p, m_p, y_p of the developed film, i.e. IP film (the subscript 'p' indicates positive). Indeed, the dye density is a linear function of the log-exposure level given by:

$$c_p = k_c + \gamma_c log_{10}(X_r) \quad (5)$$

where k_c is constant, γ_c is slope H-D curve.

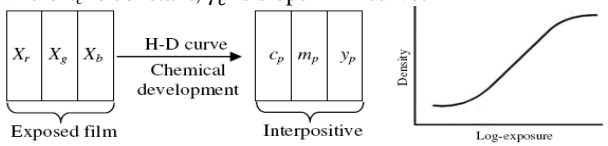

Figure 4 – From exposed film to interpostive

In the 3rd step (see Fig.5), IP is scanned to form DF. Similar to equation (2), the transmitted light $ST(\lambda)$ of the scanned light $S(\lambda)$ is obtained from Beer-Lambert law:

$$ST(\lambda) = S(\lambda)\tau_p(\lambda) \quad (6)$$

where $\tau_p(\lambda)$ is the transmittance of IP film:

$$\tau_p(\lambda) = 10^{-(c_p D_c(\lambda) + m_p D_m(\lambda) + y_p D_y(\lambda))z} \quad (7)$$

Note that, unlike color-timing light $E(\lambda)$, the scanned light $S(\lambda)$ is unchanged for all shots. This transmitted light passes through a sensor and a gamma correction step finally forms the digital images:

$$R = \left[t_1 \int_w ST(\lambda) Q_r(\lambda) d\lambda\right]^{\gamma} \quad (8)$$

where R is the digital value, $Q_r(\lambda)$ is the red sensitivity of sensor, γ the is gamma correction coefficient. In practice, Dirac delta function can be considered a tolerable approximation for most real sensors [7]. Therefore, we can replace $Q_r(\lambda)$ by $\delta(\lambda - \lambda_r)$ and (8) becomes:

$$R = [t_1 ST(\lambda_r)]^{\gamma} \quad (9)$$

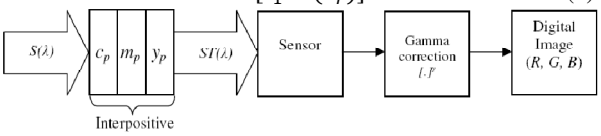

Figure 5-From interpositive to digital film

This set of equations (1-7, 9) describes the main processes undergone by the film from its ON to its DF.

3. PROPOSED MOTION ESTIMATION METHOD

To detect and restore the degraded region, it is necessary to align the degraded frame with the reference one. This could be achieved by using the motion field between them. However, motion estimation in the case of color change is a challenging task. In the literature, there are two main approaches of motion estimation: block matching and optical flow. The first one is mainly used in video coding. Indeed, it is known to be inconsistent in homogenous regions [8]. On the other hand, the second approach yields dense motion flow thanks to the smoothness motion term in its framework. Since the detection and restoration steps depend heavily on the quality of the estimated flow, the optical flow approach is chosen in this work. It is worth noticing that this method is based on two fundamental assumptions (i) small movement and (ii) brightness constancy. However, these assumptions are usually violated. To cope with large motion, coarse-to-fine scheme [9] is known to be the best solution. In the case of color variation, Golland et al.[10] propose to use normalized *rgb* values (i.e. *r=R/(R+G+B)*) to deal with global multiplicative illumination changes. In other work, Milena et al. [11] use the hue component in the HVS space to tackle the problem of highlights and specular reflection. In our case, we will show that the derivative of logarithm of digital values is invariant to color change. Let us consider the horizontal derivative of logarithm, i.e. $(logR)_i$ (we note *i* for column, *j* for line). The first derivative is approximated by the forward difference:

$$(logR)_i = \log_{10}\left(R^{(i,j)}\right) - \log_{10}\left(R^{(i+1,j)}\right) \quad (10)$$

By using equations (9,7,6), we obtain:

$$(logR)_i = \gamma z \left(CD_c(\lambda_r) + MD_m(\lambda_r) + YD_y(\lambda_r)\right)$$

where $C = c_p^{(i+1,j)} - c_p^{(i,j)}$, $M = m_p^{(i+1,j)} - m_p^{(i,j)}$, $Y = y_p^{(i+1,j)} - y_p^{(i,j)}$. From equation (5), we can derive $C = \gamma_c log_{10}\left(X_r^{(i+1,j)} / X_r^{(i,j)}\right)$ (similar results can be obtained for *M* and *Y*). Using equation (4), we have:

$$C = \gamma_c log_{10}\left(\frac{\int_w E^{(i+1,j)}(\lambda)\tau_n^{(i+1,j)}(\lambda)L_r(\lambda)d\lambda}{\int_w E^{(i,j)}(\lambda)\tau_n^{(i,j)}(\lambda)L_r(\lambda)d\lambda}\right)$$

where

$$\tau_n^{(i,j)}(\lambda) = 10^{-(c_n^{(i,j)} D_c(\lambda) + m_n^{(i,j)} D_m(\lambda) + y_n^{(i,j)} D_y(\lambda))z}$$

$$E^{(i,j)}(\lambda) = \alpha_r^{(i,j)} E_r(\lambda) + \alpha_g^{(i,j)} E_g(\lambda) + \alpha_b^{(i,j)} E_b(\lambda)$$

Note that, since red-sensitive layer $L_r(\lambda)$ of IP does not absorb blue and green components of $E(\lambda)$, we can approximate *C* as follows:

$$C \approx \gamma_c log_{10}\left(\frac{\int_w \alpha_r^{(i+1,j)} E_r(\lambda)\tau_n^{(i+1,j)}(\lambda)L_r(\lambda)d\lambda}{\int_w \alpha_r^{(i,j)} E_r(\lambda)(\lambda)\tau_n^{(i,j)}(\lambda)L_r(\lambda)d\lambda}\right)$$

Note that the weighting factor $\alpha_r^{(i,j)}$ is a function of line *j*, then $\alpha_r^{(i,j)} = \alpha_r^{(i+1,j)}$. Finally, *C* becomes:

$$C = \gamma_c log_{10}\left(\frac{\int_w E_r(\lambda)\tau_n^{(i+1,j)}(\lambda)L_r(\lambda)d\lambda}{\int_w E_r(\lambda)(\lambda)\tau_n^{(i,j)}(\lambda)L_r(\lambda)d\lambda}\right)$$

It is important to notice that the value *C* does not depend on the change of weighting factors $\alpha_r, \alpha_g, \alpha_b$. Similar remarks can be drawn for *M* and *Y*. Therefore, $(logR)_i$ is invariant to illumination change. Let us consider the vertical derivative of logarithm, i.e. $(logR)_j$. Similar equation (10), we have:

$$(logR)_j = \log_{10}\left(R^{(i,j)}\right) - \log_{10}\left(R^{(i,j+1)}\right)$$

Note that if we consider the weighting factor α_r is similar in two consecutive lines, i.e. $\alpha_r^{(i,j)} \approx \alpha_r^{(i,j+1)}$, we can draw that $(logR)_j$ is invariant to illumination too. Using the same reasoning, it is easy to see that $(logG)_i$, $(logG)_j$, $(logB)_i$ and $(logB)_j$ have similar property.

Based on these analyses, instead of using directly intensity values RGB, we propose to use the derivatives of the logarithm (*DoL*) of these values as data term in the optical flow scheme. The proposed objective function is then as follows:

$$E(u,v) = E_D(u,v) + \alpha E_S(u,v) \qquad (11)$$

where *u,v* are motion flow vectors to estimate, α is regularisation factor, $E_D(u,v)$ is the data term and $E_S(u,v)$ is the smoothness motion term defined as follows:

$$E_D(u,v) = \int_{\mathrm{i,j}\in\Omega} \left(\sum_{ch,dir} \psi\left(DoL_{ch,dir}^{deg}(i+u, j+v) - DoL_{ch,dir}^{ref}(i,j) \right)^2 \right) didj$$

$$E_S(u,v) = \int_{\mathrm{i,j}\in\Omega} \psi(|\nabla u|^2 + |\nabla v|^2) didj$$

where $|\nabla.|$ is the norm of gradient, *ch* stands for channel, *dir* indicates derivative direction (so we have 3 channels –red, green, blue; and 2 derivative directions – vertical and horizontal), Ω is the image domain, *deg* and *ref* refer to degraded and reference frame, respectively. To make method more robust to outliers and preserve motion boundaries [9,11,12], we propose to use L_1-norm which is given by function $\psi(s) = \sqrt{s+\varepsilon}$. The objective function $E(u,v)$ is then minimised by solving the Euler-Lagrange equations. A coarse-to-fine strategy [9] is also used to deal with large motion.

4. DETECTION AND RESTORATION

According to our experience, the distortion never exceeds the half of the frame. Therefore, to save computational time, motion is estimated only on the haft of frame where the distortion may appear. Using the computed flow field, a warped-frame is estimated from the reference one. Note that unlike the reference frame, this warped one is now well aligned with the degraded one. To detect the extent of the degraded region, we propose to compare the Mean Intensity of each Line (*MIL*) between the degraded and warped frames. The proposed idea is based on the fact that the *MIL* for the same line of two consecutive frames does not change except in the case of color change. The *MIL* is defined as follows:

$$MIL^{ch}(j) = \sum_{i=1}^{W} I^{ch}(i,j) \Big/ W$$

where I^{ch} is the intensity of the channel *ch* (red, green, blue), *W* is the width of the frame. An absolute difference between *MIL* profiles is then computed and used as a index of color-mismatch. If the degradation is on the top of frame, we seek from left to right the first point for which the absolute difference is smaller than a threshold T_{line}. The spatial extent of the distortion is then determined from this crossover. If the degradation is on the bottom of the frame, the same reasoning is applied from left to right. Note that this process is independently carried out for each channel since the degradation differs from one to another.

In the restoration step, thanks to accurate motion, the warped values can be directly used as restored pixels. However, note that the occluded pixels in the degraded frame have no correspondence in the reference frame then they have to be isolated from unoccluded ones and restored by other way. Indeed, the occlusion can be detected based on the consistence between the forward and backward flows [12]. Note that the forward motion (the degraded frame is anchor, the reference frame is target) of an unoccluded pixel in the degraded frame is exactly opposite to the backward motion (the reference frame is anchor, the degraded frame is target) of its correspondence in the reference frame, whereas for an occluded pixel, this property is no longer true. Let denote $\left[u_f^{(i,j)}, v_f^{(i,j)}\right]$ is forward motion of pixel *(i,j)* in the degraded frame, $\left[u_b^{(i,j)}, v_b^{(i,j)}\right]$ is backward motion of pixel *(i,j)* in the reference frame. The matching error vector $\left[\rho_u^{(i,j)}, \rho_v^{(i,j)}\right]$ is defined as follows:

$$\rho_u^{(i,j)} = \left| u_f^{(i,j)} + u_b^{\left(i+u_f^{(i,j)}, j+v_f^{(i,j)}\right)} \right| \qquad (12a)$$

$$\rho_v^{(i,j)} = \left| v_f^{(i,j)} + v_b^{\left(i+u_f^{(i,j)}, j+v_f^{(i,j)}\right)} \right| \qquad (12b)$$

A pixel *(i,j)* in the degraded frame is considered occluded if the matching error vector is very large. Otherwise, it is in unoccluded region. Therefore, occluded pixels in the degraded frame can be detected by thresholding the norm of the matching error vector with a threshold T_{occ}. In our work, a supplemental dilation operator is carried to enlarge the occluded regions. The occluded pixels are thus restored by

using an interpolated function which is derived from degraded and warped pixels in the unoccluded regions.

5. EXPERIMENTAL RESULTS

The experimental results are carried out on high definition (HD) films. A degraded frame and its reference are shown in Fig.6. The color degradation appears on the top of this frame where the sky and the forest are greener than in reference one (see zooms in Fig.13, 14). To demonstrate the robustness of the proposed optical flow method, we compare it with the one obtained from the use of raw values RGB (called 'raw' method). Two forward flows are shown in Fig.7a,b. It is easy to see that, while the 'raw' method fails, the proposed one yields accurate flow even in the case of color change. This accurate flow is then used to derive the warped frame as shown in Fig.12. Note that the red regions on the right and bottom of this frame are due to occlusion resulting from global movement (camera's movement). As can be seen the zooms in Fig.13c and Fig.14b, the warped frame has the same structure as the degraded one except in the occlusion regions (around the head of the man in Fig.13c). The *MIL* profiles of the degraded and warped frames are shown in Fig.10b. Unlike *MIL* of degraded and reference frames in Fig.10a where they are misaligned, thanks to reliable motion, the *MIL* in Fig.10b are well aligned. The **c**orrelation between *MIL* of the **d**egraded frame and the **w**arped one (CDW) and that between *MIL* of the **d**egraded frame and **r**eference one (CDR) are reported in table 1. As can be seen, CDW is much higher than CDR. This clearly confirms the efficiency of the motion estimation method. Now, by thresholding the absolute difference between two aligned-MIL profiles with T_{line}=5, we can determinate the degraded region. The backward flow is illustrated in Fig.8. Based on forward and backward flows, the norm of matching error vector (see equation 12) is estimated (see Fig.11). It is easy to see that high values (indicate occlusion region) are on the right, bottom of frame and around the man. By taking T_{occ}=5, the occlusion map is obtained. The dilation of this map is shown in Fig.9. The occluded regions on the borders are due to global motion and the ones around the man are due to local motion. A function is then derived from degraded and corresponding warped pixels in the unoccluded regions. The degraded pixels in the occluded regions are thus restored by using this function. The restored frame is shown in Fig.6c and its zoomed version in Fig13.d and Fig.14c. Compared to the warped frame in Fig13.c, the occluded region around the head of the man is now correctly detected and restored. In Fig.14c, since this region is unoccluded, the restored frame directly uses the result from the warped regions. An objective evaluation based on Kullback–Leibler (KL) distance which is based on statistical information and free from motion and image structure is carried out too. A comparison of KL distance of the degraded region and the reference one (KL-DegRef) and that of the restored region and the reference one (KL-ResRef) is reported in table 2. As can be seen, while KL-DegRef is very high, KL-ResRef is nearly zeros for all channels. It means that the restored region has same tone as the reference one.

	Red channel	Green channel	Blue channel
CDW	0.9947	0.9965	0.9725
CDR	0.9154	0.9127	0.8498

Table 1: CDW/CDR comparison

	Red channel	Green channel	Blue channel
KL-DegRef	0.2792	0.1284	0.3869
KL-ResRef	0.0105	0.0079	0.0081

Table 2: KL-DegRef/KL-ResRef comparison

Please use your monitor to view the images and visit http://www-l2ti.univ-paris13.fr/~do/eusipco/index.html to get more results.

6. CONCLUSIONS

In this paper, an accurate color correction method has been proposed and tested on real film sequences. A physical model describing the main processes undergone by the film from its original state to its digital form is the proposed and validated through the obtained results. A new optical flow based on this physical model has been also derived. It is shown that the proposed motion estimation method is robust to illumination change. The flow field is then used for detecting and restoring the image. The whole proposed color correction scheme is objectively and subjectively evaluated. The obtained results clearly demonstrate the efficiency of the proposed solutions.

REFERENCES

[1] R.E. Jacobson, S.F. Ray, G.G. Attridge and N.R. Axford, *The manual of photography: photographic and digital imaging*, 9th edition, Focal Press, 2000.

[2] D. Case, *Film Technology in Post Production*, 2nd edition, Focal Press, 2001.

[3] G. Kennel, *Color and mastering for digital cinema*, Focal Press, 2007.

[4] Q.B. Do, M. Luong, A. Beghdadi, "Detection and restoration of color-timing echo artifact for HD digital cinema films," International Conference on Image Processing ICIP, pp. 3585 – 3588, 2010.

[5] W. Smith, *Modern optical engineering: The design of opitical systems*, 4th edition, McGraw-Hill, 2007.

[6] Kodak: The essential reference guide for filmmakers-2010. Avaible on http://motion.kodak.com.

[7] G. Finlayson, S. Hordley, "Color constancy at a pixel," Journal of the Optical Society of America A: Optics, Image Science, and Vision, vol.18, pp. 253-264, 2001.

[8] C. Liu and W.T. Freeman, "A high-quality video denoising algorithm based on reliable motion estimation," in European Conference on Computer Vision, 2010.

[9] T. Brox, A. Bruhn, N. Papenberg and J. Weickert, "High accuracy optical flow estimation based on a theory for warping", ECCV, vol.4, pp. 25-36, 2004.

[10] P. Golland and A.M. Bruckstein, "Motion from color," Computer Vision and Image Understanding, vol. 68, pp. 356-362, 1997.

[11] Y. Mileva, A. Bruhn, J. Weickert, "Illumination-robust variational optical flow with photometric invariants," In DAGM-Symposium, LNCS 4713, pp.152-162, 2007.

[12] S. Ince and J. Konrad, "Geometry-based estimation of occlusions from video frame pairs," International Conference on Acoustics, Speech, and Signal Processing, vol. 2, pp. 933-936, 2005.

Figure 6 – from left to right (a) the degraded frame, (b) the reference frame, (c) the restored frame

Figure 7 – from left to right (a) forward motion flow of proposed method, (b) forward motion flow of 'raw" method (see text), (c) motion color code: hue indicates orientation and saturation indicates magnitude

Figure 8 – Backward motion flow of proposed method

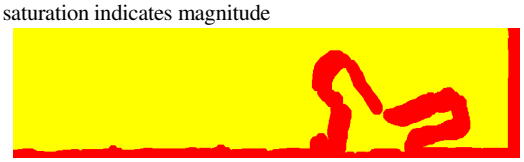

Figure 9 – Dilated occlusion map (yellow indicates unoccluded region, red indicates occluded region

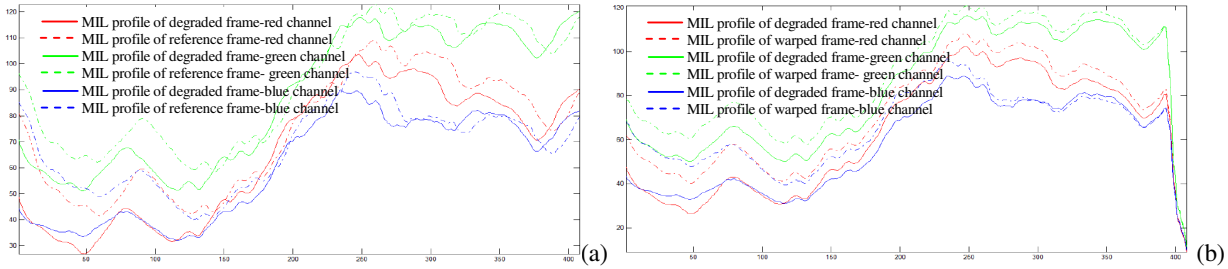

Figure 10 – from left to right (a) MIL of degraded frame & reference frame, (b) MIL of degraded frame & warped frame

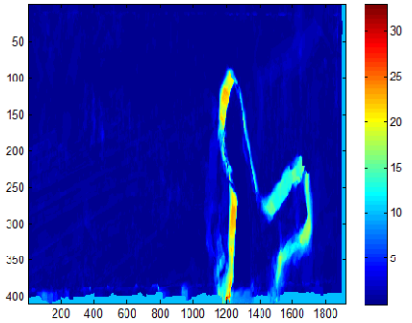

Figure 11 – Norm of matching error vector (see equation 12)

Figure 12 –Warped frame estimated from forward motion flow and the reference frame

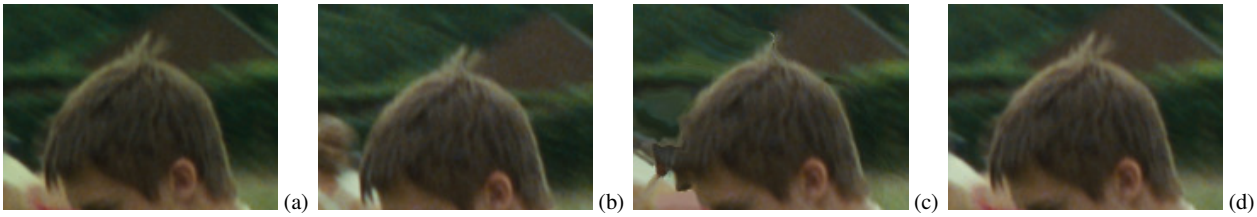

Figure 13 – from left to right (a) zoom of degraded frame, (b) zoom of reference frame, (c) zoom of warped frame (d) zoom of restored frames

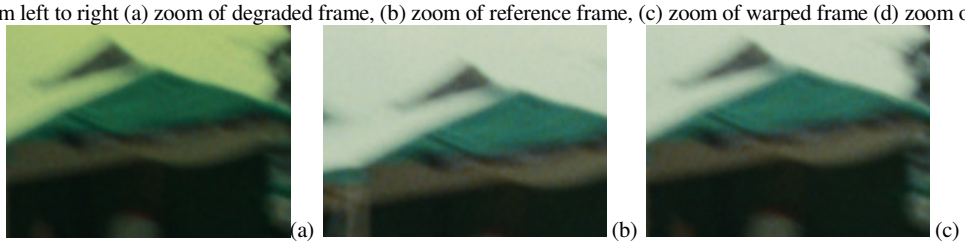

Figure 14 – from left to right (a) zoom of degraded frame, (b) zoom of reference frame, (c) zoom of warped and restored frames